

Virtual Screening for Submicromolar Leads of tRNA-guanine Transglycosylase Based on a New Unexpected Binding Mode Detected by Crystal Structure Analysis

Ruth Brenk,[†] Lars Naerum,^{‡,§} Ulrich Grädler,^{†,||} Hans-Dieter Gerber,[†] George A. Garcia,[⊥] Klaus Reuter,[†] Milton T. Stubbs,[†] and Gerhard Klebe^{*,†}

Institut für Pharmazeutische Chemie, Philipps-Universität Marburg, Marbacher Weg 6, 35032 Marburg, Germany, NovoNordisk A/S, Novo Allé, 2880 Bagsvaerd, Denmark, and Interdepartmental Program in Medicinal Chemistry, College of Pharmacy, University of Michigan, Ann Arbor, Michigan 48109-1065

Received July 12, 2002

Eubacterial tRNA-guanine transglycosylase (TGT) is involved in the hypermodification of cognate tRNAs, leading to the exchange of G34 by preQ1 at the wobble position in the anticodon loop. Mutation of the *tgt* gene in *Shigella flexneri* results in a significant loss of pathogenicity of the bacterium due to inefficient translation of a virulence protein mRNA. Herein, we describe the discovery of a ligand with an unexpected binding mode. On the basis of this binding mode, three slightly deviating pharmacophore hypotheses have been derived. Virtual screening based on this composite pharmacophore model retrieved a set of potential TGT inhibitors belonging to several compound classes. All nine tested inhibitors being representatives of these classes showed activity in the micromolar range, two of them even in the submicromolar range.

Introduction

Shigellae are the causative agents of dysentery (shigellosis) and effect more than one million deaths each year.¹ Shigellosis is usually treated by antibiotics,^{2,3} but more and more multidrug-resistant strains are reported. Accordingly, there is urgent need for the development of new antibiotics against shigellosis.⁴

Characterization of chromosomal mutants of *S. flexneri* has resulted in the identification of a gene, *vacC*, that contributes significantly to pathogenicity.⁵ The nucleotide sequence of the *vacC* gene is highly homologous (>98%) to the *tgt* gene of *Escherichia coli*, coding for tRNA-guanine transglycosylase (TGT, EC 2.4.2.29).^{6,7} TGT is involved in the biosynthesis of the highly modified nucleoside queuine (Figure 1) inserted in the anticodon loop of certain tRNAs. In eubacteria, the exchange of guanine in the unmodified tRNA by the queuine precursor preQ₁ (7-methylamino-7-deazaguanine, Figure 1) is catalyzed. Recent studies have shown that the reaction follows an associative mechanism.⁸ Once incorporated into tRNA, preQ₁ undergoes further chemical modification through at least two subsequent enzymatic steps to yield the final queuine modification.^{9,10} Although the exact biological function of modified bases in tRNAs is still unclear, it is known that particularly those present in the anticodon region can alter the efficiency and fidelity of tRNAs during translation.^{11–13} Blocking the biological function of TGT with specific inhibitors is expected to result in tRNAs

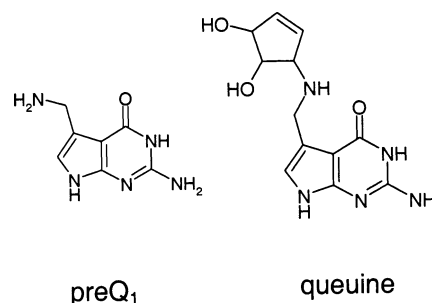


Figure 1. Chemical structures of preQ₁ and queuine.

lacking queuine in the anticodon. In *S. flexneri*, this leads to significantly reduced expression of the *virF* gene, which in consequence results in a dramatic reduction of virulence.^{6,14}

The crystal structure of *Zymomonas mobilis* TGT has been solved at 1.85 Å.¹⁵ The residues participating in substrate binding and catalysis of *Z. mobilis* TGT are identical with those of the *S. flexneri* enzyme apart from the replacement of Tyr106 by a phenylalanine residue.¹⁶ Therefore, the crystal structure of *Z. mobilis* TGT provides an ideal platform for the rational design of potent inhibitors against shigellosis.

Structure-based drug design is an iterative cycle.¹⁷ The process starts with a detailed analysis of the binding site of the target protein, which is preferably complexed with a ligand. This complex unravels the binding mode and conformation of a ligand under investigation and indicates the essential aspects determining its binding affinity. It is then used to generate new ideas about ways of improving an existing ligand or of developing new alternative bonding skeletons. Computational methods supplemented by molecular graphics are applied to assist this step of hypothesis generation. The features of the protein binding pocket can be translated into queries used for virtual computer

* To whom correspondence should be addressed. Phone: 0049 6421 2821313. Fax: 0049 6421 2828994. E-mail: klebe@mail.uni-marburg.de.

[†] Philipps-Universität Marburg.

[‡] NovoNordisk A/S.

[§] Present address: Combio A/S, Gamle Carlsberg Vej 10, 2500 Valby, Denmark.

^{||} Present address: ALTANA-Pharma, Byk-Gulden-Strasse 2, 78467 Konstanz, Germany.

[⊥] University of Michigan.

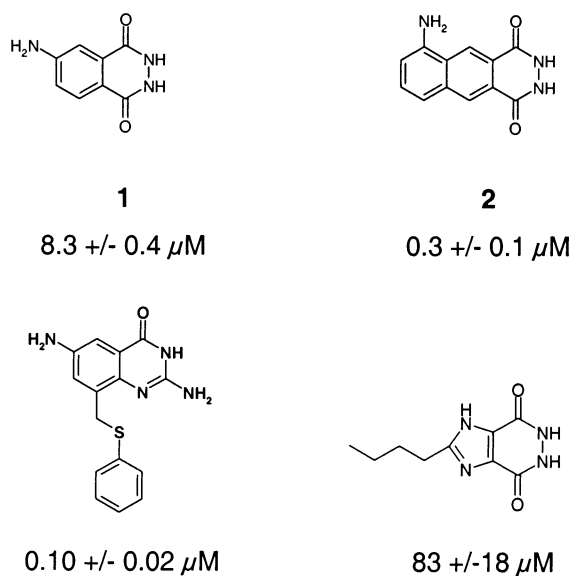


Figure 2. Compounds used in the test set with K_i values.

73 screening of large compound libraries or to design novel
74 ligands de novo. These initial proposals must be con-
75 firmed experimentally. Subsequently, they are opti-
76 mized toward higher affinity and selectivity.

77 In a recent design study, 4-aminophthalhydrazide (**1**)
78 was found to be an inhibitor of TGT.¹⁸ Its binding mode
79 was determined crystallographically. Starting from this
80 structure, here we present the next design cycle using
81 X-ray crystallography, “hot spot” analysis, and virtual
82 screening techniques.

83 Results and Discussion

84 In a previous de novo design study, we discovered
85 pyridazinedione derivatives, e.g. **1** and **2** (Figure 2), as
86 possible inhibitors of TGT in the low micromolar to
87 submicromolar range.¹⁸ Attempts to improve binding
88 affinity by placing additional substituents of polar
89 nature into the neighborhood of the two facing Asp102
90 and Asp280 residues did not result in better binding.
91 We explained this finding by repulsive interactions of
92 an uncharged triazole substituent bound to the parent
93 benzopyridazinedione skeleton. This substituent has
94 been found to be disordered in the crystal structure of
95 the protein–ligand complex. Furthermore, the assumed
96 repulsive interactions lead to a rupture of the hydrogen
97 bond formed between the exocyclic NH_2 group of the
98 parent structure and the backbone carbonyl group of
99 Leu231. On the basis of these findings, we concluded
100 that this hydrogen bond is an important feature for
101 strong ligand binding. This assumption is further sup-
102 ported by a recent study based on substituted 2-amino-
103 3*H*-quinazoline-4-ones to accommodate the guanine
104 binding site. Synthesis of derivatives possessing or
105 lacking the described exocyclic NH_2 group results in a
106 more than 10-fold affinity difference.¹⁹ To further study
107 the structural properties of pyridazinediones, we screened
108 the proprietary NovoNordisk Compound Database
109 (NNCD) for corresponding analogues using traditional
110 2D substructure searching and a combined search
111 strategy.²⁰ From these computer searches, the com-
112 pounds shown in Table 1 were selected and tested. First
113 attempts to dock these compounds into the binding site
114 of TGT suggested a structural inadequacy apart from

Table 1. List of Five Pyridazinediones Retrieved in the NNCD and Tested for TGT Inhibition

No	Compound	K_i [μ M]
3		5.0 +/- 1.2
4		4.7 +/- 1.0
5		36 +/- 11
6		83 +/- 18
7		200 +/- 70

5. None of these inhibitors appeared capable of hydrogen-
bonding to the important backbone carbonyl of Leu231.
We were surprised that all compounds showed inhibi-
tory activity in the micromolar range. **3** and **4** even
inhibited the enzyme with low micromolar affinity
(Table 1).

For crystals of the *Z. mobilis* TGT, a soaking system
with a good solvent-accessible binding site is estab-
lished.^{15,21} Therefore, we tried to soak the different
compounds into crystals of TGT to collect evidence for
this rather unexpected good binding affinity. Successful
soaking could be achieved in the case of the well-soluble
6. Unexpectedly, the crystal analysis of this complex
shows a flip of the peptide bond at Ala232 to Leu231
(Figures 3 and 4). This flip rotates the carbonyl group
of Leu231 out from the binding pocket. The adjacent
NH of Ala232 is now facing the ligand binding site. The
side chain of Leu231 virtually remains in the same
position. Furthermore, an interstitial water molecule
(W1) is incorporated, thus mediating a firm contact to
the backbone NH of Ala232 and the imidazole nitrogen
of **6** (Figure 4). In addition, this water molecule is
hydrogen-bonded to the sulfur of Cys158. A water
molecule at this site has not yet been observed in any
other ligand complex with *Z. mobilis* TGT or the apo
structure. It exhibits a B factor of only 34.8 \AA^2 , which
is in the same range as the B factors for the adjacent
ligand atoms. This may be taken as a crude indicator
for full occupancy and rather strong binding. In addi-
tion, fewer dramatic changes are also observed. The side
chain of Gln107 moves slightly toward the ligand, now
giving rise to a hydrogen bond to a second interstitial
water molecule (W2), which mediates further contact
to the ligand. The quite unexpected coincidence of two

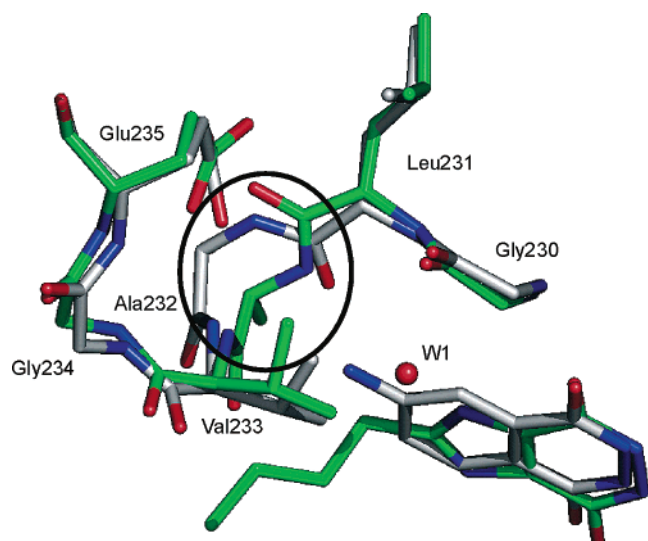


Figure 3. Superposition of a part of the protein structure of TGT in complex with **1** (green) and **6** (gray). The peptide bond at Leu231 to Ala232 (circle) in the structure of TGT complexed with **6** is flipped compared to that with **1**. The flip rotates the carbonyl group of Leu231 off from the binding pocket. The adjacent NH of Ala232 is now facing the ligand-binding site. The side chain of Leu231 remains at virtually the same position. (Picture has been produced using PyMOL.)

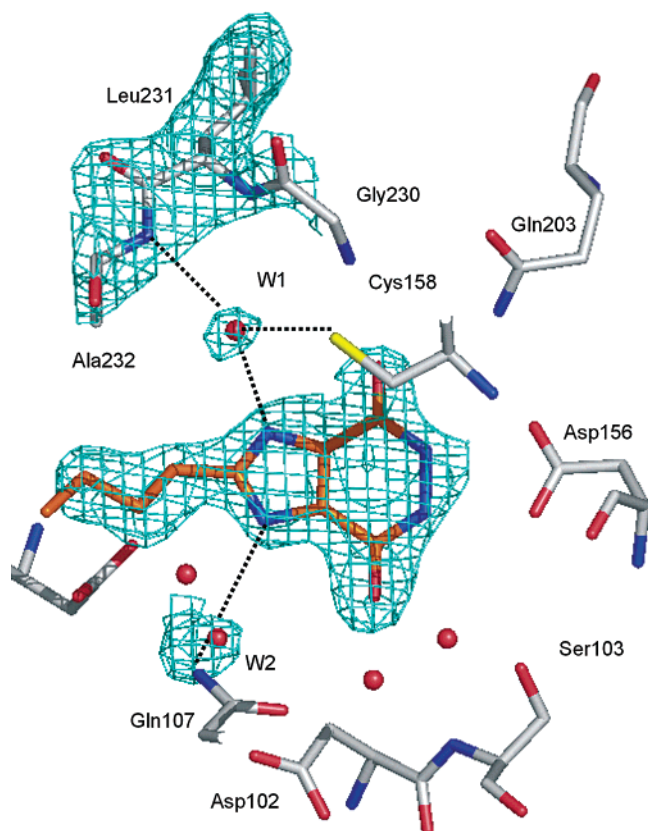


Figure 4. Representation of the 2.1 Å resolution $|F_o| - |F_c|$ simulated annealing omit map contoured at 3.0σ of the *Z. mobilis* TGT in complex with **6**. (Picture has been produced using PyMOL.)

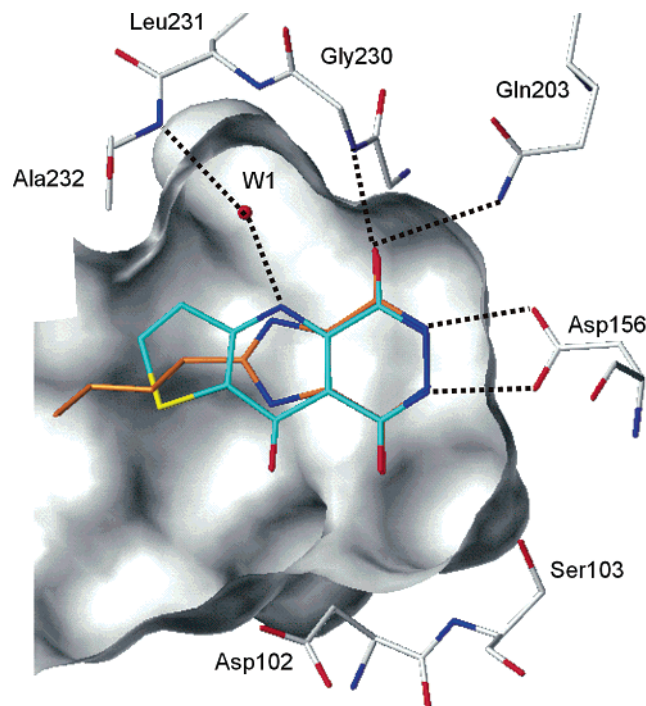


Figure 5. Modeled binding mode of **3** (cyan). The crystallographically determined binding mode of **6** (orange) is shown for comparison. Both ligands can form hydrogen bonds to Asp156, Gln203, and Gly230 as well as to the interstitial water molecule W1, which mediates the contact to Leu231. (Picture has been produced using SYBYL.)

complexes are already characterized. It also underlines the importance of crystal structure analysis as a prerequisite for successful iterative structure-based design. On the basis of the crystal coordinates of the complex with **6**, the binding modes of **3**, **4**, and **7** have been modeled accordingly. The suggested binding mode of **3** as a representative example is shown in Figure 5.

The discovery of this new binding geometry resulting from an obvious plasticity of the protein in this region inspired us to develop a structure-based pharmacophore hypothesis for virtual screening comprising the different binding modes, as evidenced by crystal structure analysis (Figure 6). First, we considered the hydrogen-bonding pattern as discovered in the complexes with **1** and **2**, in particular since the protein conformer with the exposed backbone carbonyl of Leu231 that accepted a hydrogen bond from the ligand is supposed to contribute strongly to binding.¹⁸ In the newly discovered protein conformer with **6**, an interstitial water operates as mediator. Because this water molecule W1 is obviously tightly bound in the complex, it was included in the search query, thus allowing for a higher variability of potential ligands. Owing to their ambivalent hydrogen-bonding properties, water molecules can operate in principle either as donors or as acceptors. Therefore, to complement the hydrogen-bonding facilities of this water, potential ligands can exhibit a donor or acceptor group at this site (Figure 6). Most of our presently discovered tight binding inhibitors expose one acceptor facility toward Gly230 and Gln203 and two donor properties toward Asp156 in a bifurcated hydrogen-bonding pattern.^{18,22} Therefore, these features have also been incorporated in our pharmacophore hypothesis.

ligand-induced structural rearrangements of the binding site would have been impossible to predict on the basis of the previous structural knowledge of TGT binding. It clearly demonstrates the inherent limitations of predicting binding modes even if several ligand-protein

154
155
156
157
158
159
160
161
162
163
164
165
166
167
168
169
170
171
172
173
174
175
176
177
178
179
180
181
182
183
184
185
186

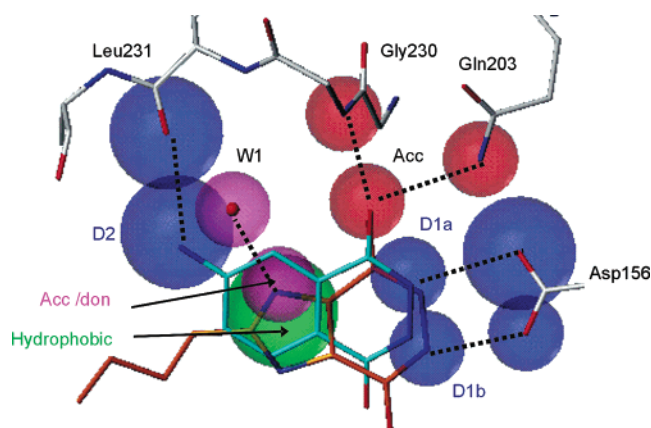


Figure 6. Structure-based pharmacophore hypothesis. The interaction to the carbonyl group of Leu231 is considered rather than the interaction to the water molecule W1. Requested donor features and the corresponding acceptor-site features of the protein are in blue, acceptor features and the corresponding donor-site features of the protein are in red, the acceptor/donor feature and the corresponding donor/acceptor site feature of the water molecule are in magenta, and the hydrophobic feature is in green. (Picture has been produced using SYBYL.)

187 To manifest these qualitative considerations of binding
 188 features on a more quantitative basis, we performed
 189 a “hot-spot” analysis using several probe functional
 190 groups in SuperStar²³ and DrugScore.²⁴ We have al-
 191 ready successfully applied this strategy in the search
 192 for new inhibitors of human carbonic anhydrase II.^{25,26}
 193 SuperStar is a method for identifying interaction sites
 194 in protein binding pockets based entirely on experimen-
 195 tal information about nonbonded interactions derived
 196 from the statistical analysis of packing patterns in
 197 crystal structures of small molecules. DrugScore is
 198 based on data derived from crystal structures of ligand-
 199 protein complexes and translates the frequency of
 200 particular protein-ligand contacts into atom/atom-pair
 201 preferences. In SuperStar, which explicitly considers
 202 the orientation of hydrogen atoms, the water molecule W1
 203 was handled as a hydrogen-bond acceptor or donor. In
 204 DrugScore, which ignores the actual protonation states
 205 of functional groups of both the protein and the ligand,
 206 the water molecule was assigned to an O.3-type oxygen.
 207 The results of these analyses are shown in Figure 8.
 208 Figure 8a shows the “hot spots” calculated with Drug-
 209 Score for an N.3 probe (ligand donor group) for the
 210 binding pocket complexed with **1** (Figure 6). Figure 8b
 211 depicts similar information for the binding pocket with
 212 the flipped backbone conformation present in the TGT·
 213 **6** complex (Figure 7b). Direct comparison of the two
 214 maps clearly demonstrates the shift of the donor “hot
 215 spot” from the region where the amino group of **1** is
 216 found toward a site where the imidazole nitrogen of **6**
 217 is located after the water molecule has been incorpo-
 218 rated. Figure 8c shows the “hot spots” for a ligand
 219 acceptor functional group using the pocket with the
 220 flipped backbone conformation (Figure 7c). The map
 221 has been calculated using SuperStar. In this analysis,
 222 the water W1 has been considered as a hydrogen-bond
 223 donor with respect to the ligand probe. Both situations,
 224 parts b and c of Figure 7, take the ambivalent donor/
 225 acceptor property of the interstitial water molecule into
 226 account. In consequence, a complementary acceptor or

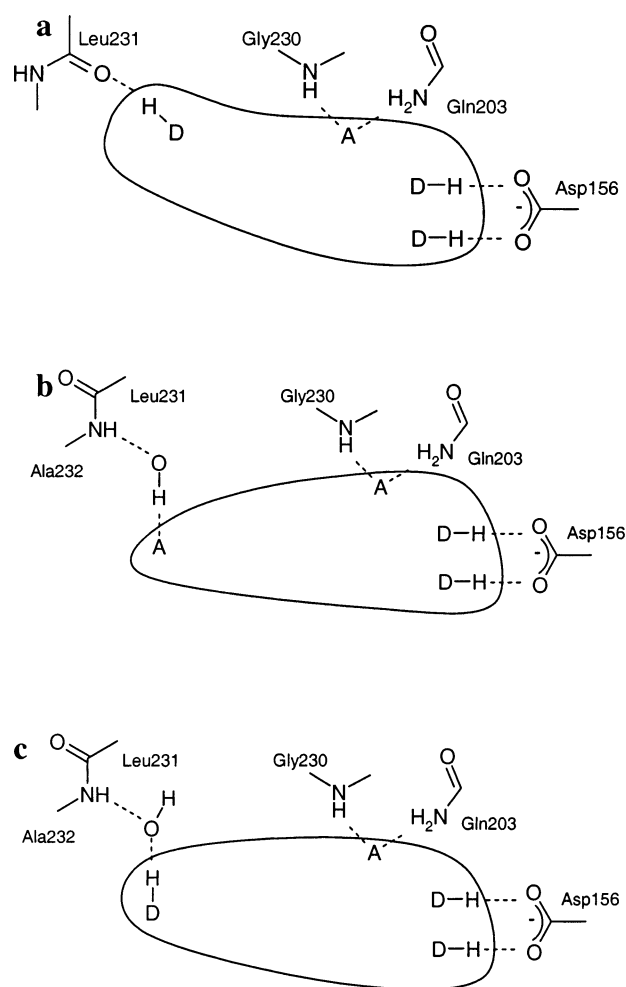


Figure 7. Schematic view of the different backbone conformations in the binding site of TGT, and the hydrogen-bond pattern considered in the pharmacophore hypothesis: (a) backbone conformation of the binding pocket complexed with **1**; (b) backbone conformation of the binding pocket complexed with **6**, with the interstitial water molecule exposing its donor property toward the ligand; (c) backbone conformation of the binding pocket complex with **6**, with the water molecule now exposing its acceptor property toward the ligand. “A” indicates an acceptor group, and “D” indicates a donor group.

227 donor functionality is required in a putative ligand at
 228 this site. Figure 8d presents the “hot spots” for a
 229 hydrophobic C.ar probe atom calculated with DrugScore.
 230 Again, the “hot spot” coincides well with the placement
 231 of the aromatic ring in **6** found in the crystal structure.

232 In the following, the above-described “hot spot” areas
 233 for the different probes, “hydrogen-bond donor”, “hy-
 234 drogen-bond acceptor”, and “hydrophobic aromatic prop-
 235 erty”, have been translated into a search query appro-
 236 priate for Unity²⁷ following the protocol described by
 237 Grüneberg et al.²⁶ The various search-tolerance spheres
 238 have been placed by picking the appropriate atoms of
 239 **1**, compared with the atoms of **6**, and their diameters
 240 have been adjusted to the spread of the indicated “hot
 241 spots” (Figure 6).

242 In our previous study, we limited the virtual screening
 243 to a subset of the ACD. In the present study, we
 244 extended our retrieval to eight different databases
 245 containing in total over 800 000 candidate molecules.

246 The screening has been performed in a stepwise
 247 fashion using Selector,²⁸ Unity, and FlexX²⁹ and in-

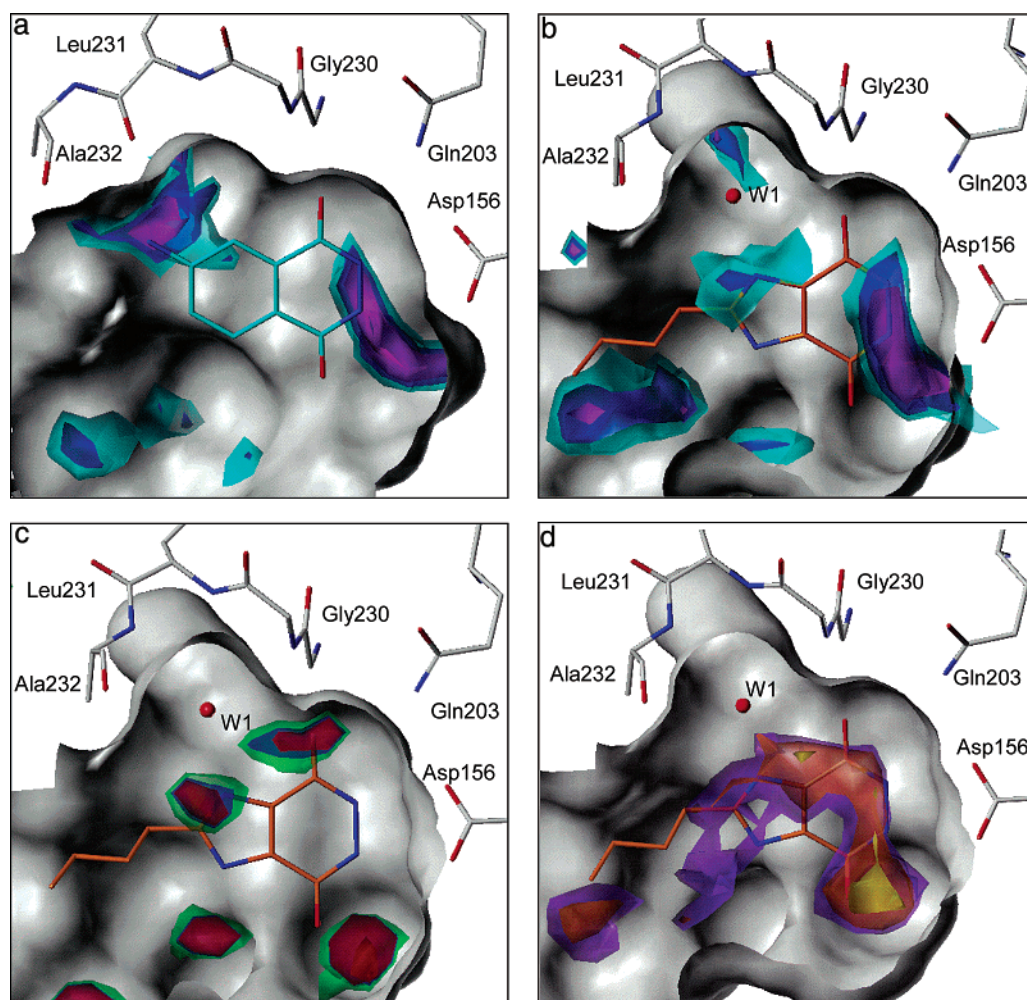


Figure 8. Mapping of putative binding “hot spots” in the active-site of TGT. For orientation, the binding geometry of the inhibitor **1** or **6**, studied crystallographically, is also shown: (a, b) highlighting of the properties of a putative hydrogen-bond donor group in a ligand, with DrugScore with N.3, contoured on 80% (cyan), 84% (blue), and 88% (magenta) levels with respect to the global minimum, for (a) the binding pocket of TGT in complex with **1** and (b) the binding pocket of TGT in complex with **6**; (c) highlighting of the properties of a putative hydrogen-bond acceptor group in a ligand, with SuperStar with a carbonyl oxygen probe, contoured at relative propensity levels of 4 (green), 8 (blue), and 10 (red), in which a propensity level of 1 corresponds to random occurrence; (d) highlighting of the properties of a putative hydrophobic probe in a ligand, with DrugScore using C.ar, contoured at 89% (magenta), 91% (orange), and 95% (yellow). (Pictures have been made using SYBYL.)

248 included several hierarchical filters of increasing complex-
 249 ity with respect to their computational requirements.²⁶
 250 In a fast initial step, only compounds with up to seven
 251 rotatable bonds and a molecular weight of less than 450
 252 Da have been considered. The reasons for these criteria
 253 are (a) to avoid highly flexible ligands and (b) to retrieve
 254 hits small enough to allow for further optimization, thus
 255 focusing on “leadlike” hits.^{30,31} Almost 50% of the
 256 compounds were eliminated by this rather unspecific
 257 and target-independent filter. In a second step, limiting
 258 the database to compounds comprising at least (a) two
 259 hydrogen-bond donors, (b) one hydrogen-bond acceptor,
 260 and (c) one hydrophobic moiety further reduced the
 261 candidate molecules to about 20% of the initial set. The
 262 protein-based pharmacophore hypothesis has been used
 263 in the third step to constrain the directionality and
 264 mutual spatial arrangement of the required hydrogen
 265 bonds and the hydrophobic moiety. In a fourth step, in
 266 addition to the criteria of the previous one, the ap-
 267 proximate shape of the binding site has been considered
 268 in terms of excluded volume constraints. The final hit
 269 list contained 872 compounds. Accordingly, the hierar-

chical filtering procedure reduced the databases to only
 0.11% of their original size (Table 2). Sixteen dupli-
 cates have been discarded because of multiple occur-
 rences in the eight databases of deviating origin that
 obviously contain slightly overlapping information.

Out of these 856 compounds, 130 passed all the filters
 because they can form a direct hydrogen bond with the
 carbonyl oxygen of Leu231, as found in the crystal
 structure of TGT·**1**. An amount of 726 hits were re-
 trieved because of their ability to form a hydrogen bond
 with the interstitial water molecule W1, underlying the
 importance of including this water in the query.

The hit list contained compounds of several different
 chemical classes, e.g., 120 carboxylic acid hydrazides
 directly attached to an aromatic ring moiety, 33 car-
 boxylic acid hydrazides attached to an aliphatic carbon,
 75 guanine derivatives, 61 hydroxyaminopiperidines,
 43 pyrazolylamines or pyrazoles, and 20 pterins. Some
 selected examples are given in Figure 9.

Subsequently, the obtained hit list was inspected
 visually. Prospective hits were then docked into one of
 the two alternative binding site conformations of the

270
 271
 272
 273
 274
 275
 276
 277
 278
 279
 280
 281
 282
 283
 284
 285
 286
 287
 288
 289
 290
 291

Table 2. Statistical Overview of the Results from Sequential Application of a Series of Hierarchical Filters on the Eight Considered Databases

filter step	ACD ^a		Ambinter ^a		Ambinter Nat ^a		AEGC ^a	
	no. of compds	%	no. of compds	%	no. of compds	%	no. of compds	%
1. rotatable bonds/MW	215212	100.00	114855	100.00	960	100.00	182485	100.00
2. requested no. of hydrophobic donor and acceptor properties	135502	62.96	59580	51.87	297	30.94	91677	50.24
3. pharmacophore hypothesis	41626	19.34	26164	22.78	120	12.50	39068	21.41
3.1. discarded because of timed out ^b	1223	0.57	496	0.43	0	0.00	591	0.32
4. excluded volumes	202	0.09	316	0.28	1	0.10	392	0.21
4.1. discarded because of timed out ^b	478	0.22	118	0.10	0	0.00	75	0.04
	128	0.06	55	0.05	0	0.00	115	0.06

filter step	AEPC ^a		ChemStar ^a		IBS ^a		LeadQuest ^a		Σ	
	no. of compds	%	no. of compds	%	no. of compds	%	no. of compds	%	no. of compds	%
	44549	100.00	57927	100.00	158942	100.00	52022	100.00	826952	100.00
1.	9417	21.14	28712	49.57	76321	48.02	18231	35.04	419737	50.76
2.	5890	11.65	12466	21.52	35661	22.44	8093	15.56	168387	20.36
3.	67	0.15	169	0.29	699	0.44	64	0.12	3309	0.40
3.1 ^b	18	0.04	0	0.00	328	0.21	19	0.04	1276	0.15
4	31	0.07	39	0.07	128	0.08	3	0.01	872	0.11
4.1 ^b	6	0.01	45	0.08	152	0.10	7	0.01	508	0.06

^a Release dates: ACD, 2000; AMBINTER, 2001; AEGC, AEPC, ChemStar, and IBS, 2001; Leadquest, 2000. ^b The main reasons that the compounds could not be placed within the time limit were that they had many rotatable bonds and/or many functional groups, e.g., sugars.

292 TGT as found in the complex with **1** or **6**, using FlexX.
 293 Ligands that still matched the pharmacophore hypothesis
 294 after docking were minimized with the MAB force
 295 field³² while keeping the binding pocket rigid. A final
 296 selection for purchase and enzyme testing included the
 297 following criteria: (a) the overall matching of the
 298 requested hydrogen-bonding network, (b) complemen-
 299 tarity between ligand and protein surfaces in terms of
 300 spatial occupancy and matched contacts in hydrophobic/
 301 hydrophilic surface patches, and (c) the absence of
 302 unfavorable van der Waals interactions after minimiza-
 303 tion.

304 For the retrieved hits **8–16**, enzyme inhibition has
 305 been characterized. Interestingly enough, all compounds
 306 displayed activities in the micromolar range or higher
 307 (Table 3).

308 For the pterin-derivatives (**8–10**), a binding mode
 309 very similar to that of **6**, considering the mediating
 310 water molecule, can be assumed. 6-Methylpterin (**8**) is
 311 the most potent compound discovered, with a K_i value
 312 of 0.2 μM . Pterin (**9**) falls into the same range ($K_i = 0.6$
 313 μM). The latter hit has already been tested in eucaryotic
 314 TGT, with a K_i of 90 nM being reported.³³ The third
 315 pterin derivative (**10**, 7-phenylpterin) exhibits a K_i value
 316 of 3.8 μM . The reduced affinity of **10** compared to **8** and
 317 **9** is probably due to the fact that the molecule has to
 318 adopt an unfavorable conformation in the binding
 319 pocket. The optimal torsion angle between the phenyl
 320 ring and the pterin moiety is about 40°. However, if this
 321 conformation is adopted in the binding pocket, the
 322 planar stacking between the pterin moiety and Tyr106
 323 would be disturbed because of close contacts with the
 324 adjacent 7-phenyl ring of the ligand. Accordingly, the
 325 ligand is most likely forced to adopt a less favorable
 326 virtually planar conformation.

327 Pyrazolylamines (**11** and **12**) are a newly detected
 328 class of TGT inhibitors. Compared to the natural
 329 substrate preQ₁, which exhibits a K_M of 0.2 μM ,³⁴ they

are rather weak binders. This is probably a consequence
 of the fact that, compared to preQ₁, the acceptor group
 is not an exocyclic carbonyl function but an aromatic
 nitrogen. Depending on the tautomeric form (Figure 10),
 this nitrogen can either be an acceptor (**12**) or carry a
 hydrogen and thus act as a donor (**12a**), which would
 be unfavorable for binding. This “unfavoured” tautomer
 (**12a**), however, appears to be the significantly more
 stable tautomeric form, as indicated by quantum chemi-
 cal calculations carried out for compound **12**. Accord-
 ingly, the compound may predominantly exist in a form
 that precludes tight binding and would actually have
 been discarded by the pharmacophore filter once
 considered as this tautomeric form in the search. In
 addition, the pyrazolylamine tautomer **12** providing the
 correct hydrogen-bonding pattern does not ideally fulfill
 the requirements for tight interaction. The distance
 between the acceptor group and the two donor groups,
 which are exposed to Gly230-NH, Gln203-NH₂, or
 Asp156, appears much shorter, thus supposedly not
 ideally matching the required hydrogen-bonding pattern
 defined by the protein. In consequence, extended hy-
 drogen bonds to Glu203 and Gly230 might result. These
 two aspects taken together may explain the reduced
 binding affinity.

Open-chain carboxylic acid hydrazides constitute a
 second new compound class. The K_i value of **13** falls into
 the same range as those of **5** and **6**. Compared to **5** and
6, the carboxylic acid hydrazides are easily accessible
 via substitution of the free carboxylic acids or esters.³⁵
 Numerous esters and acids are commercially available.
 Accordingly, **13** might serve as a prospective lead
 structure for further optimization. In addition, open-
 chain hydrazides are already known as drugs; for
 example, isoniazid is a well-known drug for the treat-
 ment of tuberculosis. It is even administered to children
 without observation of serious side effects over a period
 of up to half a year.³⁶

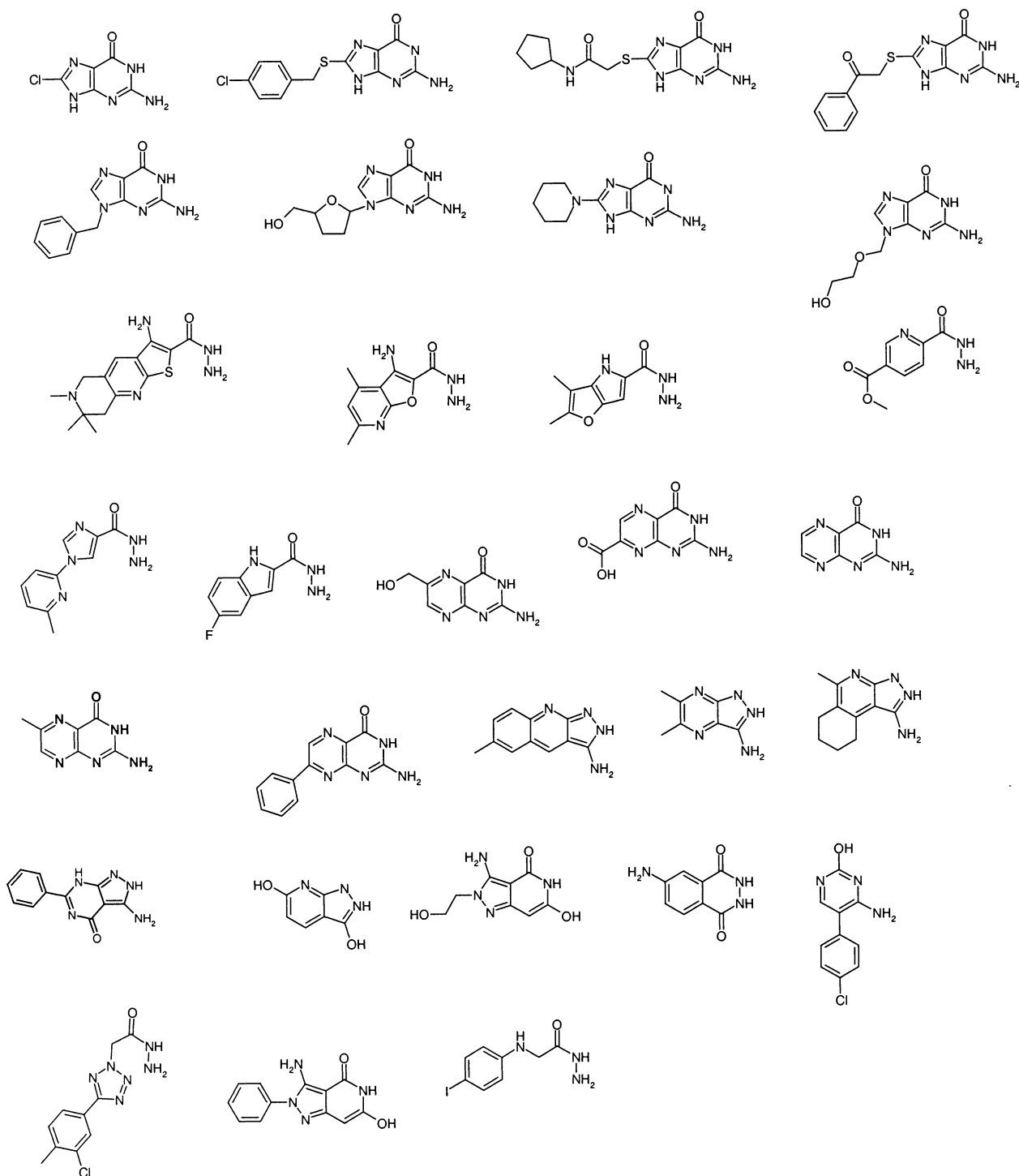


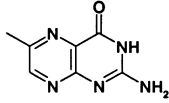
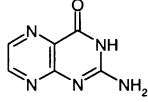
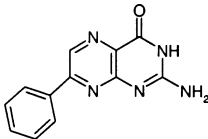
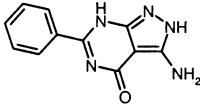
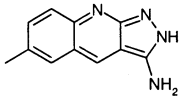
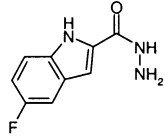
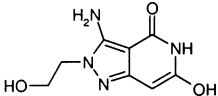
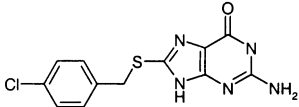
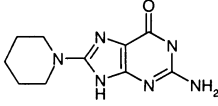
Figure 9. Selected hits discovered by virtual screening.

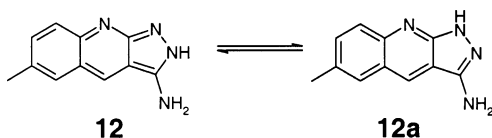
368 Hit **14** is the first inhibitor discovered that most likely
 369 exposes a hydroxyl group to Asp156. The second OH
 370 group in the side chain appears suitable as a linker for
 371 the attachment of molecular portions that could possibly
 372 interact with additional amino acid residues in the
 373 active site distal from the substrate recognition site.

374 Compounds **15** and **16** are substituted guanines.
 375 Guanine itself, which is accepted by the TGT as a
 376 substrate, exhibits a K_M of $0.7 \mu\text{M}$.³⁷ The K_I of **16**
 377 is about 1.5 orders of magnitude higher, probably because
 378 of steric crowding next to the directly connected piperi-
 379 dine moiety, while the K_I for **15** ($2.7 \mu\text{M}$) is in the range
 380 of the K_m for guanine. Up to now, we could report on

two studies focused on structure-based design of TGT 381
 inhibitors.^{18,22} In both studies, attempts were made to 382
 improve affinity by adding appropriate side chains that 383
 possibly interact with the polar functional groups of 384
 amino acid residues Asp280, Asp102, and Asn70 or fill 385
 the adjacent small hydrophobic cleft formed by Val45, 386
 Leu68, and Val282. For these studies, molecular skel- 387
 etons derived from either the benzpyridazinedione- or 388
 2-amino-3H-quinazolinone type were selected. In 389
 both cases, side chains have been added to the core 390
 structure in the 6-position instead of in the 8-position. 391
 Compound **15** is the first lead discovered with a side 392
 chain attached in a topologically different orientation 393

Table 3. List of the Nine Compounds Discovered by Virtual Screening That Were Subsequently Selected for TGT Inhibition Testing

No	Compound	Database	Label	K _i [μM]
8		ACD	MFCD00012137	0.25 +/- 0.05
9		ACD / IBS	MFCD00010557 / STOCK1N-11489	0.6 +/- 0.2
10		ACD	MFCD02091220	3.8 +/- 0.1
11		ACD	MFCD00110262	249 +/- 47
12		AEPC	ASN2538273	156 +/- 36
13		ACD	MFCD01566929	72 +/- 5
14		AEGC	BAS0316634	8.1 +/- 1.0
15		AEPC	ASN3578296	2.7 +/- 0.3
16		AEGC	BAS0449619	37 +/- 7

**Figure 10.** Tautomeric forms of pyrazolamines.

394 (Figure 11). It is thus expected that this molecule
 395 experiences new sites of interactions in the binding
 396 pocket of TGT. A promising affinity in the low micro-
 397 molar range has been detected for this compound, thus
 398 indicating that these additional interactions could fa-
 399 vorably contribute to ligand binding.

400 Conclusions

401 We have discovered a new, unexpected binding mode
 402 of a novel TGT inhibitor. Owing to the flip of a binding
 403 site exposed peptide bond, the originally presented

backbone carbonyl group becomes buried while the 404
 donor functionality of the adjacent backbone NH is now 405
 presented for ligand binding. In addition, a water 406
 molecule is incorporated, thus mediating a favorable 407
 ligand–protein interaction. This hardly predictable 408
 behavior underlies the importance of crystal structure 409
 analysis as a prerequisite for successful iterative struc- 410
 ture-based drug design. The new binding mode has been 411
 considered along with the ambivalent donor/acceptor 412
 properties of the interstitial water molecule to perform 413
 hydrogen-bonding to a putative ligand in order to define 414
 three slightly deviating pharmacophore hypotheses. 415
 Virtual screening based on this composite pharmaco- 416
 phore model retrieved a set of potential TGT inhibitors 417
 emerging from several compound classes. Out of these, 418
 nine inhibitors have been selected for experimental 419
 testing. All retrieved compounds show activity in the 420

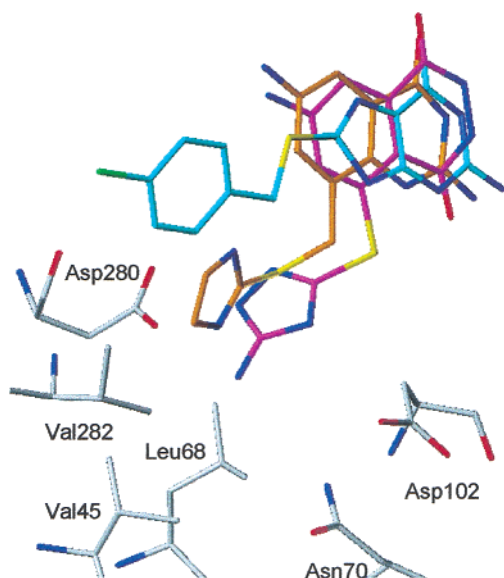


Figure 11. Assumed binding mode of **15** (cyan) compared to the crystallographically determined binding modes of two already characterized inhibitors (orange²² and magenta¹⁸). (Picture has been produced using SYBYL.)

421 micromolar range, and two even exhibit submicromolar
422 inhibition. Some of the newly discovered ligand skel-
423 etons are currently being investigated as a starting
424 point for further lead optimization.

425 Experimental Section

426 Molecular modeling was performed using SYBYL 6.7³⁸ and
427 MAB/Moloc 01/05/08³⁹ running on a Silicon Graphics O2
428 (R10000) workstation.

429 **Structure Determination.** The TGT was expressed, purified,
430 and crystallized as described elsewhere.^{37,40} Crystals have
431 been soaked overnight with the inhibitor as described by
432 Grädler et al.¹⁸ X-ray data (Table 4) were collected at -173
433 $^{\circ}\text{C}$ as described.¹⁸ Diffraction data were processed using the
434 programs DENZO and SCALEPACK.⁴¹ The structure was
435 refined through several cycles of least-squares refinement
436 along with an energy minimization using CNS.⁴² Manual
437 adjustments to the electron density have been performed using
438 O.⁴³

439 **"Hot Spot" Analysis of the Binding Pocket.** "Hot Spots"
440 have been calculated using SuperStar²³ and DrugScore²⁴ as
441 alternative methods. Both programs have been applied with
442 default settings. Calculations have been performed using
443 either the unoccupied binding pocket of TGT in its conforma-
444 tion found with the bound ligand **1** (1ENU) or in the conforma-
445 tion with **6**. For SuperStar, which in contrast to DrugScore
446 explicitly considers hydrogen atoms, the hydrogens of the
447 water molecule W1 have been orientated in the binding pocket
448 to expose their hydrogen-bond acceptor or hydrogen-bond
449 donor property toward the ligand. For DrugScore, the water
450 molecule W1 has been assigned to an O.3-type oxygen. In
451 SuperStar, a carbonyl oxygen probe was selected to analyze
452 hydrogen-bond acceptor interactions, the uncharged amino
453 nitrogen probe was selected to analyze hydrogen-bond donor
454 interactions, and the aromatic CH carbon probe was selected
455 to analyze hydrophobic interactions. In DrugScore, the O.2,
456 N.3, and C.ar probe atoms have been selected accordingly.

457 **Structure-Based Pharmacophore Generation.** The crys-
458 tal structures of **6** and **1** (1ENU) in complex with TGT have
459 been superimposed by a least-squares fit based on the C_{α}
460 positions. The donor features D1a and D1b indicated in Figure
461 6 have been defined using Unity 4.2²⁷ by picking the appropri-
462 ate atoms of **6**. The acceptor (acc) feature Acc and the donor
463 (don) feature D2 have been defined by picking the appropriate
464 atoms of **1**. The acc and don features have been defined by

Table 4. Crystallographic Data and Refinement Statistics of the TGT Complex with **6**

	C2
space group	C2
cell constants	
<i>a</i> (Å)	91.06
<i>b</i> (Å)	64.38
<i>c</i> (Å)	70.77
β (deg)	96.5
resolution (Å)	30–2.1
total no. of reflections	87,053
no. of unique reflections	23,882
completeness of all data (%) (outer shell (%))	99.8 (99.4)
R_{symm} for all data ^a (outer shell (%))	9.5 (30.2)
R_{free} ^b (%)	23.3
R factor ^b (%)	18.8
no. of protein atoms (non-hydrogen atoms)	2902
no. of water molecules	282
rms deviation of angle (deg)	1.209
rms deviation of bond (Å)	0.005
average <i>B</i> factor of protein atoms (Å ²)	26.0
average <i>B</i> factor of water atoms (Å ²)	33.1
average <i>B</i> factor of ligand atoms (Å ²)	32.4

^a $R_{\text{symm}} = \sum |I - \langle I \rangle| / \sum I$, where *I* is the observed intensity and $\langle I \rangle$ is the average intensity for multiple measurements. ^b The R_{free} (ref 54) was calculated from a random selection of reflections constituting ~10% of the data. The R factor was calculated with the remaining intensities.

465 connecting a donor atom and an acceptor atom that have been
466 located by picking the appropriate atom of **6** via the partial
467 match utility. To consider the directionality of the hydrogen
468 bonds, corresponding sites have been attributed to the neigh-
469 boring atoms of the protein and the interstitial water molecule.
470 The hydrophobic moiety has been spatially characterized as
471 the centroid of the benzoic ring of **1**. D2 and the acc/don feature
472 as well as the connection of acc to Gly230 and Glu203 have
473 been connected by the partial match utility (Figure 6). The
474 receptor site has been defined by picking the appropriate atoms
475 of binding pocket. A spatial constraint has been added to all
476 features. The diameters of the features on the ligand site have
477 been set to the spread of the indicated "hot spots". The
478 diameters for the feature spheres on the protein site have been
479 adjusted in such a way that a test sample composed of already
480 known inhibitors for the TGT (Figure 2) could pass the
481 filter.^{18,22}

482 **Construction of 3D Databases.** The 2D connection tables
483 of entries in the Available Chemicals Directory (ACD),⁴⁴ IBS
484 Library,⁴⁵ ChemStar Library,⁴⁶ ASINEX Express Gold Collec-
485 tion (AEGC), ASINEX Express Platinum Collection (AEPC),⁴⁷
486 LeadQuest,⁴⁸ and AMBINTER⁴⁹ have been converted into 3D
487 structures using CORINA.⁵⁰ Thereby, missing hydrogens have
488 been added and small disconnected fragments (e.g., counter-
489 ions) have been discarded. Subsequently, the generated 3D
490 structures were transferred into Unity databases by applying
491 the Unity utility dpimport followed by the standard 2D and
492 macrofingerprint generation based on dbmkscreen.²⁷

493 **Hierarchical Filtering.** First, the databases have been
494 screened by applying the Selector compound filtering utility²⁸
495 to retrieve compounds with less than eight rotatable bonds
496 and a molecular weight of less than 450 Da. The obtained hit
497 lists have been further selected by applying the same utility
498 to retrieve molecules that possess at least two hydrogen-bond
499 donors, one hydrogen-bond acceptor, and one hydrophobic
500 feature (a five- or six-membered ring) in accordance to the
501 above-described requirements of the protein-derived pharma-
502 cophore. The remaining hits have been further filtered in a
503 subsequent step by Unity to match in a flexible fashion the
504 proposed pharmacophore hypothesis, first ignoring but then
505 considering excluded volume constraints assigned to the
506 adjacent active-site residues. During the former step, the
507 computing time maximally spent per structure has been
508 restricted to 180 s, and during the step considering volume
509 constraints, it was restricted to 300 s. To focus on leads that
510 are suitable for optimization,^{30,31} Lipinski's "rule of five" check
511 has been superseded. Duplicates, occasionally present in the

512 different databases, were then removed from the hit lists using
513 the Unix shell script noddups provided with Unity.

514 **Docking.** During the Unity searches, different tautomeric
515 forms have been considered. To prepare the preselected hits
516 for a final docking with FlexX,²⁹ manual corrections to obtain
517 the desired tautomeric form have been performed using
518 SYBYL. With an in-house script, exocyclic guanidino and
519 amidino groups or primary and secondary aliphatic amino
520 groups have been protonated. Similarly, phosphoric, sulfonic,
521 and carboxylic groups have been deprotonated.

522 Docking calculations were performed utilizing FlexX, ver-
523 sion 1.102. The FlexX scoring function has been used during
524 the complex construction phase. The obtained solutions were
525 reranked by DrugScore⁵¹ as implemented in FlexX. The
526 particle concept,⁵² which is capable of considering water
527 molecules during the incremental construction phase, was
528 activated. For each compound, 30 docking solutions have been
529 generated. These solutions have been checked using an in-
530 house PYTHON script to find the solution with the best score
531 that matches the original pharmacophore hypothesis. Only
532 compounds passing these criteria have been further consid-
533 ered.

534 **Force-Field Minimization and Quantum Chemical**
535 **Calculations.** Ligands have been minimized in the binding
536 pocket exhibiting the protein conformation as complexed with
537 **1** or **6** using the MAB force-field.³² The default parameters
538 have been applied, and the binding pocket has been kept rigid.

539 The quantum chemical calculations for the tautomers of
540 compound **12** have been performed with the HF method using
541 the 6-31G(d) basis set and ligand geometries optimized at the
542 same level. Gaussian 98 was used for these calculations.⁵³

543 **Kinetic Analysis.** The apparent K_i values have been
544 measured as described elsewhere.¹⁸

545 **Protein Data Bank Accession Codes.** The atomic coordi-
546 nates and structure factors for TGT-**6** have been deposited
547 in the RCSB Protein Data Bank with ID code 1N2V.

548 **Acknowledgment.** This work was supported by the
549 Deutsche Forschungsgemeinschaft (Grant KL-1204/1).
550 We thank Dr. C. Sotriffer for his help in quantum
551 chemical calculations and C. Sohn for his assistance in
552 the X-ray measurements. We are grateful to Tripos
553 (Munich, Germany) for making the Tripos software
554 available to us and to MDL (San Leandro, CA) for a copy
555 of the ACD library.

556 References

- 557 (1) Kotloff, K.; Winickoff, J.; Ivanoff, B.; Clemens, J.; Swerdlow, D.;
558 et al. Global burden of Shigella infections: implications for
559 vaccine development and implementation of control strategies.
560 *Bull. WHO* **1999**, *77*, 651–666.
- 561 (2) Replogle, M. L.; Fleming, D. W.; Cieslak, P. R. Emergence of
562 antimicrobial-resistant shigellosis in Oregon. *Clin. Infect. Dis.*
563 **2000**, *30*, 515–519.
- 564 (3) Khan, W. A.; Seas, C.; Dhar, U.; Salam, M. A.; Bennish, M. L.
565 Treatment of shigellosis: V. Comparison of azithromycin and
566 ciprofloxacin. A double-blind, randomized, controlled trial. *Ann.*
567 *Intern. Med.* **1997**, *1*, 697–703.
- 568 (4) Overcoming Antimicrobial Resistance. World Health Report on
569 Infectious Diseases. [http://www.who.int/infectious-disease-report/](http://www.who.int/infectious-disease-report/2000/index.html)
570 [2000/index.html](http://www.who.int/infectious-disease-report/2000/index.html) (accessed 2000).
- 571 (5) Okada, N.; Sasakawa, C.; Tobe, T.; Yamada, M.; Nagai, S.; et
572 al. Virulence-associated chromosomal loci of *Shigella flexneri*
573 identified by random Tn5 insertion mutagenesis. *Mol. Microbiol.*
574 **1991**, *5*, 187–195.
- 575 (6) Durand, J. M.; Dagberg, B.; Uhlin, B. E.; Bjork, G. R. Transfer
576 RNA modification, temperature and DNA superhelicity have a
577 common target in the regulatory network of the virulence of
578 *Shigella flexneri*: the expression of the virF gene. *Mol. Microbiol.*
579 **2000**, *35*, 924–935.
- 580 (7) Okada, N.; Nishimura, S. Isolation and characterization of a
581 guanine insertion enzyme, a specific tRNA transglycosylase,
582 from *Escherichia coli*. *J. Biol. Chem.* **1979**, *254*, 3061–3066.
- 583 (8) Kittendorf, J. D.; Barcomb, L. M.; Nonekowsky, S. T.; Garcia, G.
584 A. tRNA-Guanine Transglycosylase from *Escherichia coli*: Mo-
585 lecular Mechanism and Role of Aspartate 89. *Biochemistry* **2001**,
586 *40*, 14123–14133.
- (9) Slany, R. K.; Kersten, H. Genes, enzymes and coenzymes of
587 queuosine biosynthesis in procaryotes. *Biochimie* **1994**, *76*,
588 1178–1182.
- (10) Frey, B.; McCloskey, J.; Kersten, W.; Kersten, H. New function
590 of vitamin B12: cobamide-dependent reduction of epoxyqueuo-
591 sine to queuosine in tRNAs of *Escherichia coli* and *Salmonella*
592 *typhimurium*. *J. Bacteriol.* **1988**, *170*, 2078–2082.
- (11) Curran, L. Modified nucleosides in translation. In *Modification*
594 *and Editing of RNA*; American Society for Microbiology Press:
595 Washington, DC, 1998; pp 493–516.
- (12) Björk, G. R. Biosynthesis and function of modified nucleosides
597 in tRNA. In *tRNA: Structure, Biosynthesis, and Function*;
598 American Society for Microbiology Press: Washington, DC, 1995;
599 pp 165–205.
- (13) Björk, G. Stable RNA modification. In *Escherichia coli and*
601 *Salmonella: Cellular and Molecular Biology*, 2nd ed.; American
602 Society for Microbiology Press: Washington, DC, 1996; pp 861–
603 886.
- (14) Durand, J. M.; Okada, N.; Tobe, T.; Watarai, M.; Fukuda, I.; et
605 al. vacC, a virulence-associated chromosomal locus of *Shigella*
606 *flexneri*, is homologous to tgt, a gene encoding tRNA-guanine
607 transglycosylase (Tgt) of *Escherichia coli* K-12. *J. Bacteriol.*
608 **1994**, *176*, 4627–4634.
- (15) Romier, C.; Reuter, K.; Suck, D.; Ficner, R. Crystal structure of
610 tRNA-guanine transglycosylase: RNA modification by base
611 exchange. *EMBO J.* **1996**, *15*, 2850–2857.
- (16) Romier, C.; Meyer, J. E.; Suck, D. Slight sequence variations of
613 a common fold explain the substrate specificities of tRNA-
614 guanine transglycosylases from the three kingdoms. *FEBS Lett.*
615 **1997**, *416*, 93–98.
- (17) Klebe, G. Recent developments in structure-based drug design.
617 *J. Mol. Med.* **2000**, *78*, 269–281.
- (18) Grädler, U.; Gerber, H. D.; Goodenough-Lashua, D. M.; Garcia,
619 G. A.; Ficner, R.; et al. A New Target for Shigellosis: Rational
620 Design and Crystallographic Studies of Inhibitors of tRNA-
621 guanine Transglycosylase. *J. Mol. Biol.* **2001**, *306*, 455–467.
- (19) Meyer, E. A. Unpublished results.
- (20) Nærum, L.; Graedler, U.; Klebe, G. Virtual screening based on
624 tRNA-guanine transglycosylase. In *Rational Approaches to Drug*
625 *Design*; Prous Science: Barcelona, Spain, 2001; pp 400–402.
- (21) Grädler, U.; Ficner, R.; Garcia, G. A.; Stubbs, M. T.; Klebe, G.;
627 et al. Mutagenesis and crystallographic studies of *Zymomonas*
628 *mobilis* tRNA-guanine transglycosylase to elucidate the role of
629 serine 103 for enzymatic activity. *FEBS Lett* **1999**, *454*, 142–
630 146.
- (22) Meyer, E. A.; Brenk, R.; Castellano, R. K.; Furler, M.; Klebe,
632 G.; et al. De Novo Design, Synthesis, and in Vitro Evaluation of
633 Inhibitors for Prokaryotic tRNA-guanine Transglycosylase: A
634 Dramatic Sulfur Effect on Binding Affinity. *ChemBioChem* **2002**,
635 *3*, 250–253.
- (23) Verdonk, M. L.; Cole, J. C.; Taylor, R. SuperStar: a knowledge-
637 based approach for identifying interaction sites in proteins. *J.*
638 *Mol. Biol.* **1999**, *289*, 1093–108.
- (24) Gohlke, H.; Hendlich, M.; Klebe, G. Predicting binding modes,
640 binding affinities and “hot spots” for protein–ligand complexes
641 using a knowledge-based scoring function. *Perspect. Drug Discov.*
642 *Des.* **2000**, *20*, 115–144.
- (25) Grüneberg, S.; Wendt, B.; Klebe, G. Subnanomolar Inhibitors
644 from Computer Screening: A Model Study Using Human
645 Carbonic Anhydrase II. *Angew. Chem., Int. Ed.* **2001**, *40*, 389–
646 393.
- (26) Grüneberg, S.; Stubbs, M.; Klebe, G. Successful Virtual Screen-
648 ing for Novel Inhibitors of Human Carbonic Anhydrase: Strag-
649 egy and Experimental Confirmation. In press.
- (27) *Unity, Chemical Information Software*, version 4.2.1; Tripos,
651 Inc.: St. Louis, MO.
- (28) *Selector*; Tripos, Inc.: St. Louis MO.
- (29) Rarey, M.; Kramer, B.; Lengauer, T.; Klebe, G. A fast flexible
654 docking method using an incremental construction algorithm.
655 *J. Mol. Biol.* **1996**, *261*, 470–489.
- (30) Hann, M. M.; Leach, A. R.; Harper, G. Molecular complexity and
657 its impact on the probability of finding leads for drug discovery.
658 *J. Chem. Inf. Comput. Sci.* **2001**, *41*, 856–864.
- (31) Oprea, T. I.; Davis, A. M.; Teague, S. J.; Leeson, P. D. Is There
660 a Difference between Leads and Drugs? A Historical Perspective.
661 *J. Chem. Inf. Comput. Sci.* **2001**, *41*, 1308–1315.
- (32) Gerber, P. R. Charge distribution from a simple molecular orbital
663 type calculation and non-bonding interaction terms in the force
664 field MAB. *J. Comput.-Aided Mol. Des.* **1998**, *12*, 37–51.
- (33) Jacobson, K. B.; Farkas, W. R.; Katze, J. R. Presence of queuine
666 in *Drosophila melanogaster*: correlation of free pool with queuo-
667 sine content of tRNA and effect of mutations in pteridine
668 metabolism. *Nucleic Acids Res.* **1981**, *9*, 2351–2366.
- (34) Hoops, G. C.; Townsend, L. B.; Garcia, G. A. Mechanism-based
670 inactivation of tRNA-guanine transglycosylase from *Escherichia*
671 *coli* by 2-amino-5-(fluoromethyl)pyrrolo[2,3-d]pyrimidin-4(3H)-
672 one. *Biochemistry* **1995**, *34*, 15539–15544.
- 673

- 674 (35) Hiremath, S. P.; Hiremath, D. M.; Purohit, M. G. Synthesis of
675 substituted 2-(5'-oxo-thioxo-1',3',4'-oxadiazol-2'-yl)-indoles and
676 2-(5'-oxo-thioxo-1,3,4'-oxadiazol-2'-ylamino)indoles. *Indian J.*
677 *Chem., Sect. B* **1983**, *22*, 571–576.
- 678 (36) Al-Dossary, F. S.; Ong, L. T.; Correa, A. G.; Starke, J. R.
679 Treatment of childhood tuberculosis with a six month directly
680 observed regimen of only two weeks of daily therapy. *Pediatr.*
681 *Infect. Dis. J.* **2002**, *21*, 91–97.
- 682 (37) Reuter, K.; Ficner, R. Sequence analysis and overexpression of
683 the *Zymomonas mobilis* tgt gene encoding tRNA-guanine trans-
684 glycosylase: purification and biochemical characterization of the
685 enzyme. *J. Bacteriol.* **1995**, *177*, 5284–5288.
- 686 (38) SYBYL, *Chemical Information Software*, version 6.7; Tripos,
687 Inc.: St. Louis, MO.
- 688 (39) Gerber, P. R.; Muller, K. MAB, a generally applicable molecular
689 force field for structure modelling in medicinal chemistry. *J.*
690 *Comput.-Aided Mol. Des.* **1995**, *9*, 251–268.
- 691 (40) Romier, C.; Ficner, R.; Reuter, K.; Suck, D. Purification, crystal-
692 lization, and preliminary X-ray diffraction studies of tRNA-
693 guanine transglycosylase from *Zymomonas mobilis*. *Proteins*
694 **1996**, *24*, 516–519.
- 695 (41) Otwinowski, Z. *DENZO*, Yale University: New Haven, CT.
- 696 (42) Brunger, A. T.; Adams, P. D.; Clore, G. M.; DeLano, W. L.; Gros,
697 P.; et al. Crystallography & NMR system: A new software suite
698 for macromolecular structure determination. *Acta Crystallogr.,*
699 *Sect. D: Biol. Crystallogr.* **1998**, *54*, 905–921.
- 700 (43) Jones, T. A.; Zou, J. Y.; Cowan, S. W.; Kjeldgaard. Improved
701 methods for binding protein models in electron density maps
702 and the location of errors in these models. *Acta Crystallogr A*
703 **1991**, *47*, 110–119.
- 704 (44) Web site: <http://www.mdli.com>.
- 705 (45) Web site: <http://www.ibscreen.com>.
- (46) Web site: <http://www.chemstar.ru>. 706
- (47) Web site: <http://asinex.com>. 707
- (48) Web site: <http://leadquest.tripos.com>. 708
- (49) Web site: <http://www.ambinter.com>. 709
- (50) Sadowski, J.; Schwab, C. H.; Gasteiger, J. *CORINA, 3D Struc-*
710 *ture Generator*, version 2.0; University Erlangen-Nürnberg:
711 Erlangen, Germany. 712
- (51) Gohlke, H.; Hendlich, M.; Klebe, G. Knowledge-based scoring
713 function to predict protein–ligand interactions. *J. Mol. Biol.*
714 **2000**, *295*, 337–356. 715
- (52) Rarey, M.; Kramer, B.; Lengauer, T. The particle concept:
716 placing discrete water molecules during protein–ligand docking
717 predictions. *Proteins* **1999**, *34*, 17–28. 718
- (53) Frisch, M. J.; Trucks, G. W.; Schlegel, H. B.; Scuseria, G. E.;
719 Robb, M. A.; Cheeseman, J. R.; Zakrzewski, V. G.; Montgomery,
720 J. A., Jr.; Stratmann, R. E.; Burant, J. C.; Dapprich, S.; Millam,
721 J. M.; Daniels, A. D.; Kudin, K. N.; Strain, M. C.; Farkas, O.;
722 Tomasi, J.; Barone, V.; Cossi, M.; Cammi, R.; Mennucci, B.;
723 Pomelli, C.; Adamo, C.; Clifford, S.; Ochterski, J.; Petersson, G.
724 A.; Ayala, P. Y.; Cui, Q.; Morokuma, K.; Malick, D. K.; Rabuck,
725 A. D.; Raghavachari, K.; Foresman, J. B.; Cioslowski, J.; Ortiz,
726 J. V.; Stefanov, B. B.; Liu, G.; Liashenko, A.; Piskorz, P.;
727 Komaromi, I.; Gomperts, R.; Martin, R. L.; Fox, D. J.; Keith, T.;
728 Al-Laham, M. A.; Peng, C. Y.; Nanayakkara, A.; Gonzalez, C.;
729 Challacombe, M.; Gill, P. M. W.; Johnson, B. G.; Chen, W.; Wong,
730 M. W.; Andres, J. L.; Head-Gordon, M.; Replogle, E. S.; Pople,
731 J. A. *Gaussian 98*; Gaussian, Inc.: Pittsburgh, PA, 1998. 732
- (54) Bruenger, A. T. The free *R* value: a novel statistical quantity
733 for assessing the accuracy of crystal structures. *Nature* **1992**,
734 *355*, 472–474. 735
- JM0209937 736